

# Galaxy cluster angular size data constraints on dark energy

Yun Chen\*

*Department of Astronomy, Beijing Normal University, Beijing 100875, China and  
Department of Physics, Kansas State University, 116 Cardwell Hall, Manhattan, KS 66506, USA*

Bharat Ratra†

*Department of Physics, Kansas State University, 116 Cardwell Hall, Manhattan, KS 66506, USA  
(Dated: January 26, 2013)*

We use angular size versus redshift data for galaxy clusters from Bonamente et al. [1] to place constraints on model parameters of constant and time-evolving dark energy cosmological models. These constraints are compatible with those from other recent data, but are not very restrictive. A joint analysis of the angular size data with more restrictive baryon acoustic oscillation peak length scale and supernova Type Ia apparent magnitude data favors a spatially-flat cosmological model currently dominated by a time-independent cosmological constant but does not exclude time-varying dark energy.

PACS numbers: 95.36.+x, 98.80.-k

## I. INTRODUCTION

A number of lines of observational evidence support a “standard” model of cosmology with energy budget dominated by far by dark energy. Dark energy is most simply characterized as a negative-pressure substance that powers the observed accelerated cosmological expansion. It can evolve slowly in time and vary weakly in space, although current data are consistent with it being Einstein’s cosmological constant. On the other hand, some argue that the observed accelerated expansion should instead be viewed as an indication that general relativity does not accurately describe gravitational physics on large cosmological length scales. For recent reviews see [2–8]. In what follows we assume that general relativity provides an accurate description of gravitation on cosmological length scales.

There are many dark energy models under discussion. For recent discussions see [9–17], and references therein. Perhaps the most economical — and the current “standard” model — is the  $\Lambda$ CDM model [18], where the accelerated cosmological expansion is powered by Einstein’s cosmological constant,  $\Lambda$ , a spatially homogeneous fluid with equation of state parameter  $\omega_\Lambda = p_\Lambda/\rho_\Lambda = -1$  (with  $p_\Lambda$  and  $\rho_\Lambda$  being the fluid pressure and energy density). In this model the cosmological energy budget is dominated by  $\rho_\Lambda$ , with cold dark matter (CDM) being the second largest contributor. The  $\Lambda$ CDM model provides a reasonable fit to most observational constraints, although the “standard” CDM structure formation model might be in some observational trouble (see, e.g., [19, 20]).

The  $\Lambda$ CDM model has a few apparent puzzles. Prominent among these is that the needed  $\Lambda$  energy density scale is of order an meV, very small compared to the higher (cutoff) value suggested by a perhaps naive application of quantum mechanics. Another puzzle is that we happen to be observing at a time not very different from when the  $\Lambda$  energy density started dominating the cosmological energy budget (this is the “coincidence” puzzle).

If the dark energy density — that responsible for powering the accelerated cosmological expansion — slowly decreased in time (rather than remaining constant like  $\rho_\Lambda$ ), the energy densities of dark energy and nonrelativistic matter (CDM and baryons) would remain comparable for a longer period of time, and so alleviate the coincidence puzzle. Also, a slowly decreasing dark energy density, that is based on more fundamental physics at a higher energy density scale much larger than an meV, would result in a current dark energy density scale of an meV through gradual decrease over the long lifetime of the Universe. Thus a slowly decreasing dark energy density could resolve some of the puzzles of the  $\Lambda$ CDM model [21].

The XCDM parametrization is often used to describe a slowly decreasing dark energy density. In this parametrization the dark energy is modeled as a spatially homogeneous ( $X$ ) fluid with an equation of state parameter  $w_X = p_X/\rho_X$ , where  $w_X < -1/3$  is an arbitrary constant and  $p_X$  and  $\rho_X$  are the pressure and energy density of the  $X$ -fluid. When  $w_X = -1$ , the XCDM parametrization reduces to the  $\Lambda$ CDM model, which is a complete and consistent model. For any other value of  $w_X (< -1/3)$  the XCDM parametrization is incomplete as it cannot describe spatial inhomogeneity.

---

\*Electronic address: chenyun@mail.bnu.edu.cn

†Electronic address: ratra@phys.ksu.edu

geneities (see, e.g., [23]). For computational simplicity we study the  $\Lambda$ CDM parametrization only in the spatially-flat cosmological case.

If the dark energy density evolves in time, physics demands that it also be spatially inhomogeneous. The  $\phi$ CDM model — in which dark energy is modeled as a scalar field  $\phi$  with a gradually decreasing (in  $\phi$ ) potential energy density  $V(\phi)$  — is the simplest complete and consistent model of a slowly decreasing (in time) dark energy density. Here we focus on an inverse power-law potential energy density  $V(\phi) \propto \phi^{-\alpha}$ , where  $\alpha$  is a nonnegative constant [21, 24]. When  $\alpha = 0$  the  $\phi$ CDM model reduces to the corresponding  $\Lambda$ CDM case. Here we only consider the spatially-flat  $\phi$ CDM cosmological model.

It has been known for some time now that a spatially-flat  $\Lambda$ CDM model with current energy budget dominated by a constant  $\Lambda$  is largely consistent with most observational constraints (see, e.g., [25–28]). Supernovae Type Ia (SNeIa) apparent magnitude measurements (e.g., [22, 29–31]), in conjunction with cosmic microwave background (CMB) anisotropy data (e.g., [32–36]) combined with low estimates of the cosmological mass density (e.g., [37]), as well as baryon acoustic oscillation (BAO) peak length scale estimates (e.g., [38–41]) strongly suggest that we live in a spatially-flat  $\Lambda$ CDM model with nonrelativistic matter contributing a little less than 30 % of the current cosmological energy budget, with the remaining slightly more than 70 % contributed by a cosmological constant. These three sets of data carry by far the most weight when determining constraints on models and cosmological parameters.

Future data from space missions will tighten the constraints (see, e.g., [42–44]). However, at present, it is of great importance to consider independent constraints that can be derived from other presently available data sets. While these data do not yet carry as much statistical weight as the SNeIa, CMB and BAO data, they potentially can reassure us (if they provide constraints consistent with those from the better known data), or if the two sets of constraints are inconsistent this might lead to the discovery of hidden systematic errors or rule out the cosmological model under consideration.

Other data that have been used to constrain cosmological parameters include galaxy cluster gas mass fraction (e.g., [28, 45, 46]), gamma-ray burst luminosity distance (e.g., [47–50]), large-scale structure (e.g., [51–53]), strong gravitational lensing (e.g., [54–57]), and lookback time (e.g., [50, 58, 59, 61]) or Hubble parameter (e.g., [62], [63], [64], [65]) data. While the constraints from these data are much less restrictive than those derived from the SNeIa, CMB and BAO data, both types of data result in largely compatible constraints that generally support a currently accelerating cosmological expansion. This gives us confidence that the broad outlines of the “standard” cosmological model are now in place.

Angular size data have also been used to constrain cosmological parameters (see, e.g., [66–70]). In this paper we use the Bonamente et al. [1] (hereafter B06) galaxy cluster angular size versus redshift data to derive cosmological constraints. These measurements were determined from radio and X-ray observations. They have previously been used to constrain some cosmological parameters and to test the distance duality relationship of metric gravity models (see, e.g., [71–76]).

In this paper we use the B06 angular size versus redshift data to constrain cosmological models not previously considered, and to constrain other cosmological parameters in models previously considered. We show that these constraints are compatible with those derived using other data. We also do a joint analysis of this angular size data and SNeIa and BAO measurements and show that including the angular size data in the mix affects the constraints, although not greatly so as the angular size data do not yet have sufficient weight.

Our paper is organized as follows. In Sec. II we present the basic equations of the three dark energy models we study. Constraints from the B06 angular diameter distances of galaxy clusters are derived in Sec. III. In Sec. IV the BAO data and the SNeIa measurements are used to constrain the dark energy models. In Sec. V we determine joint constraints on the dark energy parameters from different combinations of data sets. Finally, we summarize our main conclusions in Sec. VI.

## II. BASIC EQUATIONS OF THE DARK ENERGY MODELS

The Friedmann equation of the  $\Lambda$ CDM model with spatial curvature can be written as

$$E^2(z; \mathbf{p}) = \Omega_{m0}(1+z)^3 + \Omega_{\Lambda} + (1 - \Omega_{m0} - \Omega_{\Lambda})(1+z)^2, \quad (1)$$

where  $z$  is the redshift,  $E(z) = H(z)/H_0$  is the dimensionless Hubble parameter where  $H_0$  is the Hubble constant, and the model-parameter set is  $\mathbf{p} = (\Omega_{m0}, \Omega_{\Lambda})$  where  $\Omega_{m0}$  is the nonrelativistic (baryonic and cold dark) matter density parameter and  $\Omega_{\Lambda}$  that of the cosmological constant. Throughout, the subscript 0 denotes the value of a quantity today. In this paper, the subscripts  $\Lambda$ ,  $X$  and  $\phi$  represent the corresponding quantities of the dark energy component in the  $\Lambda$ CDM, XCDM and  $\phi$ CDM models.

In this work, for computational simplicity, the spatial curvature is set to zero in the  $\Lambda$ CDM and  $\phi$ CDM cases. Then the Friedmann equation for the  $\Lambda$ CDM parametrization is

$$E^2(z; \mathbf{p}) = \Omega_{m0}(1+z)^3 + (1 - \Omega_{m0})(1+z)^{3(1+w_X)}, \quad (2)$$

where the model-parameter set is  $\mathbf{p} = (\Omega_{m0}, w_X)$ .

In the  $\phi$ CDM model, the inverse power law potential energy density of the scalar field adopted in this paper is  $V(\phi) = \kappa m_p^2 \phi^{-\alpha}$ , where  $m_p$  is the Planck mass, and  $\alpha$  and  $\kappa$  are non-negative constants [24]. In the spatially-flat case the Friedmann equation of the  $\phi$ CDM model is

$$H^2(z; \mathbf{p}) = \frac{8\pi}{3m_p^2}(\rho_m + \rho_\phi), \quad (3)$$

where  $H(z) = \dot{a}/a$  is the Hubble parameter, and  $a(t)$  is the cosmological scale factor and an overdot denotes a time derivative. The energy densities of the matter and the scalar field are

$$\rho_m = \frac{m_p^2}{6\pi} a^{-3}, \quad (4)$$

and

$$\rho_\phi = \frac{m_p^2}{32\pi}(\dot{\phi}^2 + \kappa m_p^2 \phi^{-\alpha}), \quad (5)$$

respectively. According to the definition of the dimensionless density parameter, one has

$$\Omega_m(z) = \frac{8\pi\rho_m}{3m_p^2 H^2} = \frac{\rho_m}{\rho_m + \rho_\phi}. \quad (6)$$

The scalar field  $\phi$  obeys the differential equation

$$\ddot{\phi} + 3\frac{\dot{a}}{a}\dot{\phi} - \frac{\kappa\alpha}{2}m_p^2\phi^{-(\alpha+1)} = 0. \quad (7)$$

Using Eqs. (3) and (7), as well as the initial conditions described in [24], one can numerically compute the Hubble parameter  $H(z)$ . In this case, the model-parameter set is  $\mathbf{p} = (\Omega_{m0}, \alpha)$ .

To use observational data to constrain cosmological models, we need various distance expressions. The coordinate distance is

$$r = \frac{c}{a_0 H_0 \sqrt{|\Omega_k|}} \text{sinn} \left[ \sqrt{|\Omega_k|} \int_0^z \frac{dz'}{E(z')} \right], \quad (8)$$

where  $\Omega_k$  is the spatial curvature density parameter and  $c$  is the speed of light, and

$$\frac{\text{sinn}(\sqrt{|\Omega_k|} x)}{\sqrt{|\Omega_k|}} = \begin{cases} \sin(\sqrt{-\Omega_k} x)/\sqrt{-\Omega_k} & (\Omega_k < 0), \\ x & (\Omega_k = 0), \\ \sinh(\sqrt{\Omega_k} x)/\sqrt{\Omega_k} & (\Omega_k > 0). \end{cases} \quad (9)$$

The luminosity distance  $d_L$  and the angular diameter distance  $d_A$  are simply related to the coordinate distance as

$$d_L = (a_0 r)(1+z), \quad (10)$$

and

$$d_A = (a_0 r)/(1+z). \quad (11)$$

### III. CONSTRAINTS FROM THE ANGULAR SIZE DATA

X-ray observations of the intracluster medium combined with radio observations of the galaxy cluster Sunyaev-Zeldovich effect allow for an estimate of the angular diameter distance (ADD)  $d_A$  of galaxy clusters. Here we use

Cluster	$z$	$d_A$ (Mpc)
Abell 1413	0.142	$780^{+180}_{-130}$
Abell 2204	0.152	$610^{+60}_{-70}$
Abell 2259	0.164	$580^{+290}_{-250}$
Abell 586	0.171	$520^{+150}_{-120}$
Abell 1914	0.171	$440^{+40}_{-50}$
Abell 2218	0.176	$660^{+140}_{-110}$
Abell 665	0.182	$660^{+90}_{-100}$
Abell 1689	0.183	$650^{+90}_{-90}$
Abell 2163	0.202	$520^{+40}_{-50}$
Abell 773	0.217	$980^{+170}_{-140}$
Abell 2261	0.224	$730^{+200}_{-130}$
Abell 2111	0.229	$640^{+200}_{-170}$
Abell 267	0.230	$600^{+110}_{-90}$
RX J2129.7+0005	0.235	$460^{+110}_{-80}$
Abell 1835	0.252	$1070^{+20}_{-80}$
Abell 68	0.255	$630^{+160}_{-190}$
Abell 697	0.282	$880^{+300}_{-230}$
Abell 611	0.288	$780^{+180}_{-180}$
ZW 3146	0.291	$830^{+20}_{-20}$
Abell 1995	0.322	$1190^{+150}_{-140}$
MS 1358.4+6245	0.327	$1130^{+90}_{-100}$
Abell 370	0.375	$1080^{+190}_{-200}$
MACS J2228.5+2036	0.412	$1220^{+240}_{-230}$
RX J1347.5-1145	0.451	$960^{+60}_{-80}$
MACS J2214.9-1359	0.483	$1440^{+270}_{-230}$
MACS J1311.0-0310	0.490	$1380^{+470}_{-370}$
CL 0016+1609	0.541	$1380^{+220}_{-220}$
MACS J1149.5+2223	0.544	$800^{+190}_{-160}$
MACS J1423.8+2404	0.545	$1490^{+60}_{-30}$
MS 0451.6-0305	0.550	$1420^{+260}_{-230}$
MACS J2129.4-0741	0.570	$1330^{+370}_{-280}$
MS 2053.7-0449	0.583	$2480^{+410}_{-440}$
MACS J0647.7+7015	0.584	$770^{+210}_{-180}$
MACS J0744.8+3927	0.686	$1680^{+480}_{-380}$
MS 1137.5+6625	0.784	$2850^{+520}_{-630}$
RX J1716.4+6708	0.813	$1040^{+510}_{-430}$
MS 1054.5-0321	0.826	$1330^{+280}_{-260}$
CL J1226.9+3332	0.890	$1080^{+420}_{-280}$

TABLE I: Angular diameter distances of galaxy clusters from B06.

the 38 ADDs of B06 to constrain cosmological parameters. These data can be found in Tables 1 and 2 of B06. For convenience, we re-collect them in Table I.

There are three sources of uncertainty in the measurement of  $d_A$ : the cluster modeling error  $\sigma_{\text{mod}}$ ; the statistical error  $\sigma_{\text{stat}}$ ; and, the systematic error  $\sigma_{\text{sys}}$ . The modeling errors are shown in Table I and the statistical and systematic errors are presented in Table 3 of B06. In our analysis here we combine these errors in quadrature. Thus, the total uncertainty  $\sigma_{\text{tot}}$  satisfies  $\sigma_{\text{tot}}^2 = \sigma_{\text{mod}}^2 + \sigma_{\text{stat}}^2 + \sigma_{\text{sys}}^2$ .

We constrain cosmological parameters by minimizing  $\chi_{ADD}^2$ ,

$$\chi_{ADD}^2(H_0, \mathbf{p}) = \sum_{i=1}^{38} \frac{[d_A^{\text{th}}(z_i; H_0, \mathbf{p}) - d_A^{\text{obs}}(z_i)]^2}{\sigma_{\text{tot},i}^2}. \quad (12)$$

Here  $z_i$  is the redshift of the observed galaxy cluster,  $d_A^{\text{th}}$  is the predicted value of the ADD in the cosmological model under consideration and  $d_A^{\text{obs}}$  is the measured value. From  $\chi_{ADD}^2(H_0, \mathbf{p})$  we compute the likelihood function  $L(H_0, \mathbf{p})$ . We then treat  $H_0$  as a nuisance parameter and marginalize over it using a gaussian prior with  $H_0 = 68 \pm 3.5 \text{ km s}^{-1} \text{ Mpc}^{-1}$  [77] to get a likelihood function  $L(\mathbf{p})$  that is a function of only the cosmological parameters of interest. The best-fit parameter values  $p^*$  are those that maximize the likelihood function and the 1, 2 and 3  $\sigma$  constraint contours are the set of cosmological parameters (centered on  $p^*$ ) that enclose 68.27, 95.45 and 99.73 %, respectively, of the

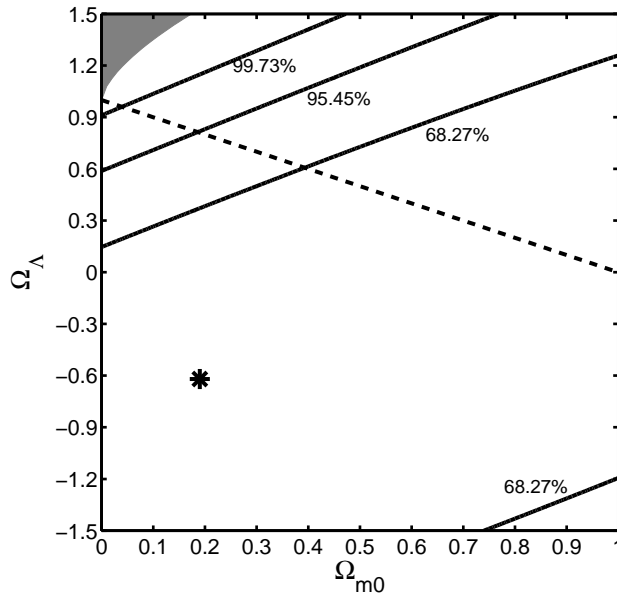


FIG. 1: 1, 2, and 3  $\sigma$  constraint contours for the  $\Lambda$ CDM model from the ADD data. The dashed diagonal line corresponds to spatially-flat models and the shaded area in the upper left-hand corner is the region for which there is no big bang. The star marks the best-fit pair  $(\Omega_{m0}, \Omega_{\Lambda}) = (0.19, -0.62)$  with  $\chi^2_{\min} = 30.1$ .

probability under the likelihood function.

Figures 1—3 show the constraints from the ADD data on the three dark energy models we consider. Comparing these results to those shown in Figs. 1—3 of [68], derived using the compact radio source angular size data of Gurvits et al. [66], and to Figs. 1—2 of [69], derived using the FRIIb radio galaxy angular size data from Guerra et al. [67], we see that the B06 galaxy cluster angular size data result in approximately comparable constraints on cosmological parameters as those from the two earlier angular size data sets. These ADD constraints are comparable to those from gamma-ray burst data ([50], Figs. 1—3 and 7—9) as well as those from Hubble parameter measurements ([63], Figs. 1—3).

Clearly, current ADD data constraints are not very restrictive, although it is encouraging that the ADD constraints on these dark energy models do not disfavor the regions of parameter space that are favored by other data. More importantly, we anticipate that near future ADD data will provide significantly more restrictive constraints on cosmological parameters.

#### IV. CONSTRAINTS FROM BAO AND SNEIA DATA

The BAO peak length scale can be used as a standard ruler to constrain cosmological parameters. Here we use the recent Percival et al. [78] BAO data to constrain parameters of the  $\Lambda$ CDM and  $\phi$ CDM models and the XCDM parametrization.

Percival et al. (2010) measure the position of the BAO peak from the SDSS DR7 and 2dFGRS data, determining  $r_s(z_d)/D_V(z = 0.275) = 0.1390 \pm 0.0037$ , where  $r_s(z_d)$  is the comoving sound horizon at the baryon drag epoch, and  $D_V(z) \equiv [(1+z)^2 d_A^2 cz/H(z)]^{1/3}$ . By using  $\Omega_{m0}h^2 = 0.1326 \pm 0.0063$  and  $\Omega_{b0}h^2 = 0.02273 \pm 0.00061$  (here  $\Omega_{b0}$  is the current value of the baryonic mass density parameter and  $h$  is the Hubble constant in units of  $100 \text{ km s}^{-1} \text{ Mpc}^{-1}$ ) from *WMAP5* [35], one can further get

$$D_V(0.275) = (1104 \pm 30) \left( \frac{\Omega_{b0}h^2}{0.02273} \right)^{-0.134} \left( \frac{\Omega_{m0}h^2}{0.1326} \right)^{-0.255} \text{ Mpc}, \quad (13)$$

as is shown in Eq. (13) of [78]. The error on  $\Omega_{b0}h^2$  is ignored in this work, as the *WMAP5* data constrains  $\Omega_{b0}h^2$  to 0.5 %.

Our results for the  $\Lambda$ CDM model and the XCDM parametrization agree very well with the Ref. [78] results shown in their Fig. 5. Our results for the  $\phi$ CDM model are shown in Fig. 4. BAO data primarily constrains  $\Omega_{m0}$  significantly,

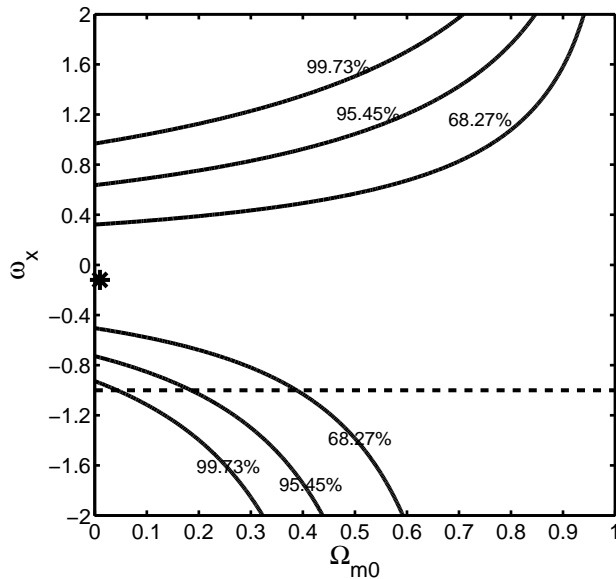


FIG. 2: 1, 2, and 3  $\sigma$  constraint contours for the XCDM parametrization from the ADD data. The dashed horizontal line at  $\omega_X = -1$  corresponds to spatially-flat  $\Lambda$ CDM models. The star marks the best-fit pair  $(\Omega_{m0}, \omega_X) = (0.01, -0.12)$  with  $\chi^2_{\min} = 30.2$ .

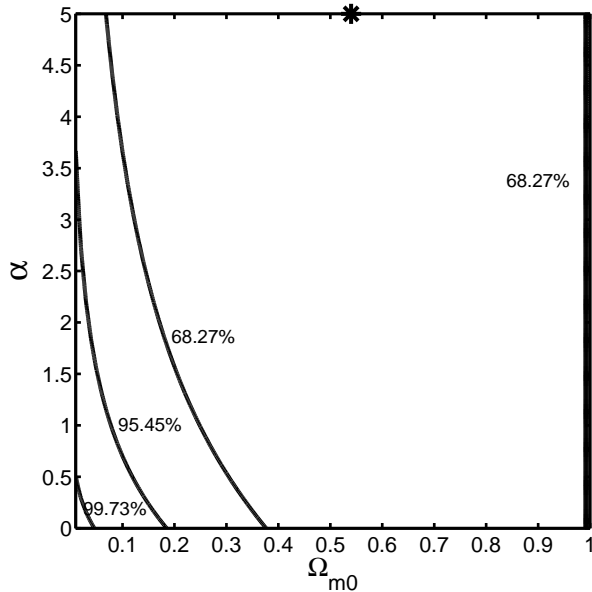


FIG. 3: 1, 2, and 3  $\sigma$  constraint contours for the  $\phi$ CDM model from the ADD data. The horizontal axis at  $\alpha = 0$  corresponds to spatially-flat  $\Lambda$ CDM models. The star marks the best-fit pair  $(\Omega_{m0}, \alpha) = (0.54, 5)$  with  $\chi^2_{\min} = 37.3$ .

leaving  $\Omega_\Lambda$ ,  $w_X$  and  $\alpha$  almost unconstrained (see, e.g., [79]). The results from the BAO data [78] are most directly comparable to those derived from the earlier BAO data of Ref. [80]. Comparing to the constraints shown in Figs. 2—4 of Ref. [79], one sees that the Percival et al. (2010) data results in slightly more restrictive constraints than the Eisenstein et al. (2005) data.

Type Ia supernovae are standardizable candles that can be used to constrain cosmological parameters. Here we use the recent Union2 compilation of 557 SNeIa (covering a redshift range  $0.015 \leq z \leq 1.4$ ) of Amanullah et al. [81] to constrain parameters of the  $\Lambda$ CDM and  $\phi$ CDM models and the XCDM parametrization.

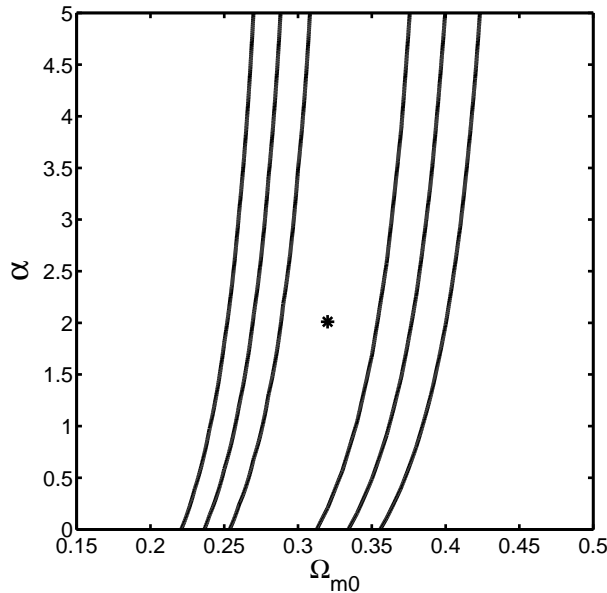


FIG. 4: 1, 2, and 3  $\sigma$  constraint contours for the  $\phi$ CDM model from the BAO data. The horizontal axis at  $\alpha = 0$  corresponds to spatially-flat  $\Lambda$ CDM models. The star marks the best-fit pair  $(\Omega_{m0}, \alpha) = (0.32, 2.01)$  with  $\chi^2_{\min} = 0.169$ .

Cosmological constraints from SNeIa data are obtained by using the distance modulus  $\mu(z)$ . The theoretical (predicted) distance modulus is

$$\mu_{\text{th}}(z; \mathbf{p}, \mu_0) = 5 \log_{10}[D_L(z; \mathbf{p})] + \mu_0, \quad (14)$$

where  $\mu_0 = 42.38 - 5 \log_{10} h$  and the Hubble-free luminosity distance is given by

$$D_L(z; \mathbf{p}) = \frac{H_0}{c} d_L = (1+z) \int_0^z \frac{dz'}{E(z'; \mathbf{p})}. \quad (15)$$

The best-fit values of cosmological model parameters can be determined by minimizing the  $\chi^2$  function

$$\chi^2_{SN}(\mathbf{p}, \mu_0) = \sum_{i=1}^{557} \frac{[\mu_{\text{th},i}(z_i; \mathbf{p}, \mu_0) - \mu_{\text{obs},i}(z_i)]^2}{\sigma_{\mu_i}^2}, \quad (16)$$

where  $\mu_{\text{obs},i}(z_i)$  is the distance modulus obtained from observations and  $\sigma_{\mu_i}$  is the total uncertainty of the SNeIa data. The zero-point  $\mu_0$  is treated as a nuisance parameter and marginalized over analytically [82–84]. The covariance matrix with or without systematic errors can be found on the web (<http://supernova.lbl.gov/Union>).

Our results for the  $\Lambda$ CDM model and the XCDM parametrization agree very well with the Ref. [81] results shown in their Figs. 10 and 11. The constraints on  $\phi$ CDM model parameters from these data are shown in Fig. 5. Comparing to Fig. 4 of Ref. [40], we see that the constraints from the Ref. [81] data with systematic errors are approximately comparable to those from the earlier Ref. [85] data for 307 SNeIa without systematic errors. Like the case for the BAO data, the SNeIa data constraints are also fairly one dimensional, tightly constraining one combination of the cosmological parameters while only weakly constraining the “orthogonal” combination.

## V. JOINT CONSTRAINTS

Figures 6–8 show the constraints on the cosmological parameters for the  $\Lambda$ CDM and  $\phi$ CDM models and the XCDM parametrization from a joint analysis of the BAO and SNeIa data, as well as from a joint analysis of the BAO, SNeIa and ADD data. With the inclusion of systematic errors in the analysis of the SNeIa data of Ref. [81], the new joint BAO and SNeIa constraints (thin solid contours in Figs. 6–8) are similar to the earlier ones shown in Figs. 4–6 of Ref. [50] that made use of the smaller SNeIa data set of Ref. [85] that did not include systematic errors.

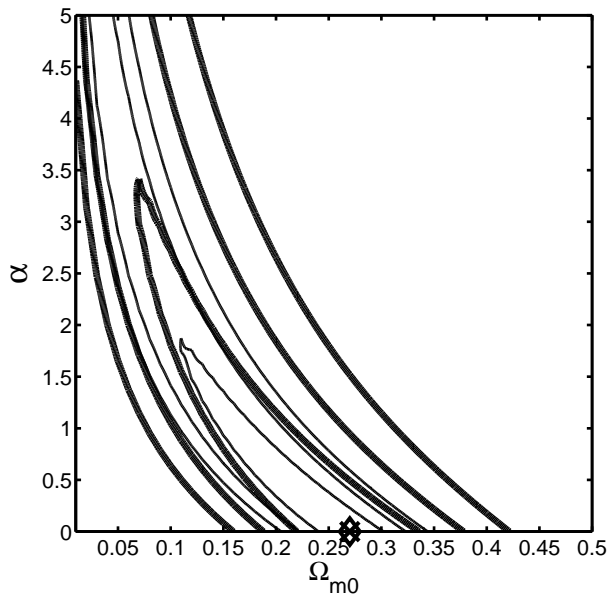


FIG. 5: 1, 2, and 3  $\sigma$  constraint contours for the  $\phi$ CDM model from the SNeIa data. The horizontal axis at  $\alpha = 0$  corresponds to spatially-flat  $\Lambda$ CDM models. Thin solid lines (best fit at  $\Omega_{m0} = 0.27$  and  $\alpha = 0.0$  with  $\chi^2_{\min} = 543$ , marked by “ $\times$ ”) exclude systematic errors, while thick solid lines (best fit at  $\Omega_{m0} = 0.27$  and  $\alpha = 0.0$  with  $\chi^2_{\min} = 531$ , marked by “ $\diamond$ ”) account for systematics.

Model	BAO + SNeIa	ADD + BAO + SNeIa
$\Lambda$ CDM	$0.24 < \Omega_{m0} < 0.33$	$0.24 < \Omega_{m0} < 0.33$
	$0.5 < \Omega_{\Lambda} < 0.97$	$0.46 < \Omega_{\Lambda} < 0.93$
XCDM	$0.24 < \Omega_{m0} < 0.33$	$0.24 < \Omega_{m0} < 0.33$
	$-1.30 < \omega_X < -0.80$	$-1.25 < \omega_X < -0.77$
$\phi$ CDM	$0.24 < \Omega_{m0} < 0.33$	$0.24 < \Omega_{m0} < 0.33$
	$0 < \alpha < 0.73$	$0.01 < \alpha < 0.89$

TABLE II: Two standard deviation bounds on cosmological parameters.

Figures 9—11 display the one-dimensional marginalized distribution probabilities of the cosmological parameters for the three cosmological models considered in this work, derived from a joint analysis of the BAO and SNeIa data, as well as from a joint analysis of the BAO, SNeIa and ADD data. The marginalized 2  $\sigma$  intervals of the cosmological parameters are presented in Table II.

The combination of BAO and SNeIa data gives tight constraints on the cosmological parameters. Adding the currently-available galaxy cluster ADD data to the mix does shift the constraint contours, however the effect is not large. Current ADD data do not have enough weight to significantly affect the combined BAO and SNeIa results. The ADD data have approximately the same weight as currently-available gamma-ray burst luminosity measurements ([50], Figs. 4—6 and 10—12).

Clearly, the observational data considered here are very consistent with the predictions of a spatially-flat cosmological model with energy budget dominated by a time-independent cosmological constant. However, the data do not rule out time-evolving dark energy, although they do require that it not vary rapidly.

## VI. CONCLUSION

We have shown that the galaxy cluster angular size versus redshift data of Ref. [1] can also be used to constrain dark energy model cosmological parameters. The resulting constraints are compatible with those derived from other current data, thus strengthening support for the current “standard” cosmological model. The ADD constraints are approximately as restrictive as those that follow from currently available gamma-ray burst luminosity data, strong gravitational lensing measurements, or lookback time (or Hubble parameter) observations. They are, however, much



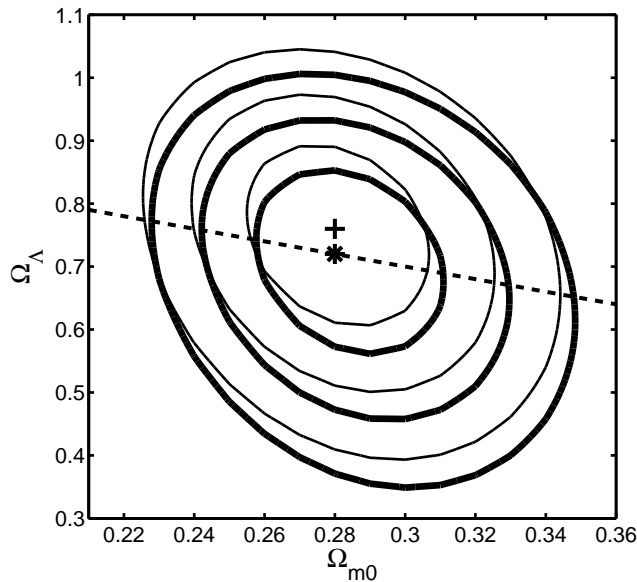


FIG. 6: Thick (thin) solid lines are 1, 2, and 3  $\sigma$  constraint contours for the  $\Lambda$ CDM model from a joint analysis of the BAO and SNeIa (with systematic errors) data, with (and without) the ADD data. The cross (“+”) marks the best-fit point determined from the joint sample without the ADD data at  $\Omega_{m0} = 0.28$  and  $\Omega_{\Lambda} = 0.76$  with  $\chi^2_{\min} = 531$ . The star (“\*”) marks the best-fit point determined from the joint sample with the ADD data at  $\Omega_{m0} = 0.28$  and  $\Omega_{\Lambda} = 0.72$  with  $\chi^2_{\min} = 565$ . The dashed sloping line corresponds to spatially-flat models.

less restrictive than those that follow from a combined analysis of BAO peak length scale and SNeIa apparent magnitude data.

The spatially-flat  $\Lambda$ CDM model, currently dominated by a constant cosmological constant, provides a good fit to the data we have studied here. However, these data do not rule out a time-evolving dark energy.

We anticipate that near-future angular size data will provide significantly more restrictive constraints on cosmological parameters. In conjunction with other observations, this angular size data will prove very useful in pinning down parameter values of the “standard” cosmological model.

### Acknowledgments

Yun Chen thanks Rodrigo Holanda, Zong-Hong Zhu and Lado Samushia for their generous and helpful advice. YC was supported by the China State Scholarship Fund No. 2010604111 and the Ministry of Science and Technology national basic science program (project 973) under grant No. 2007CB815401. BR was supported by DOE grant DEFG03-99EP41093.

- 
- [1] M. Bonamente, et al. , *Astrophys. J* 647 (2006) 25-54.
  - [2] J. A. Frieman, in: *American Institute of Physics Conference Series*, volume 1057 of *American Institute of Physics Conference Series*, pp. 87-124.
  - [3] B. Ratra, M. S. Vogeley, *Publ. Astron. Soc. Pac.* 120 (2008) 235-265.
  - [4] R. R. Caldwell, M. Kamionkowski, *Annual Review of Nuclear and Particle Science* 59 (2009) 397-429.
  - [5] M. Sami, *Curr. Sci.* 97 (2009) 887.
  - [6] M. Bartelmann, *Reviews of Modern Physics* 82 (2010) 331-382.
  - [7] Y.-F. Cai, et al. , *Physics Reports* 493 (2010) 1-60.
  - [8] P. Brax, arXiv:0912.3610
  - [9] H. Wei, *Phys. Lett. B* 695 (2011) 307-311.
  - [10] M. Jamil, E. N. Saridakis, *JCAP* 7 (2010) 28.
  - [11] M. Maggiore, *Phys. Rev. D* 83 (2011) 063514.

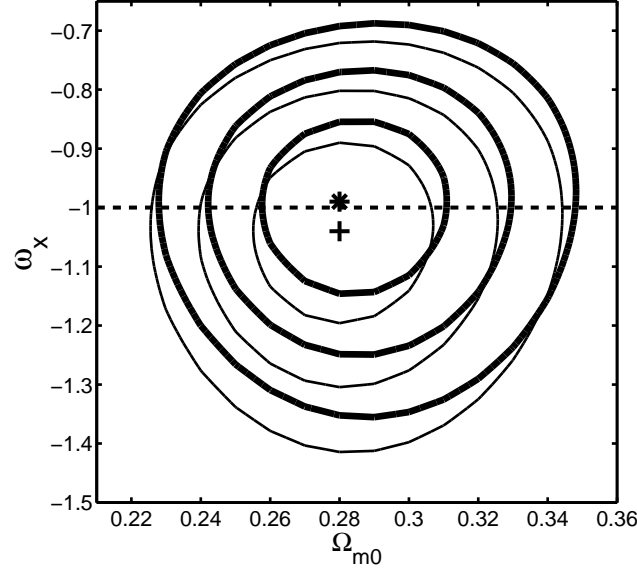


FIG. 7: Thick (thin) solid lines are 1, 2, and 3  $\sigma$  constraint contours for the XCDM parametrization from a joint analysis of the BAO and SNeIa (with systematic errors) data, with (and without) the ADD data. The cross (“+”) marks the best-fit point determined from the joint sample without the ADD data at  $\Omega_{m0} = 0.28$  and  $\omega_X = -1.04$  with  $\chi^2_{\min} = 531$ . The star (“\*”) marks the best-fit point determined from the joint sample with the ADD data at  $\Omega_{m0} = 0.28$  and  $\omega_X = -0.99$  with  $\chi^2_{\min} = 565$ . The dashed horizontal line at  $\omega_X = -1$  corresponds to spatially-flat  $\Lambda$ CDM models.

- [12] S. Dutta, R. J. Scherrer, Phys. Rev. D 82 (2010) 043526.
- [13] S.-H. Shao, P. Chen, Phys. Rev. D 82 (2010) 126012.
- [14] S. Lepe, F. Pe na, European Physical Journal C 69 (2010) 575-579.
- [15] M. S. Sloth, International Journal of Modern Physics D 19 (2010) 2259- 2264.
- [16] D.-J. Liu, Phys. Rev. D 82 (2010) 063523.
- [17] L. Lopez Honorez, et al. , JCAP 9 (2010) 29.
- [18] P. J. E. Peebles, Astrophys. J 284 (1984) 439-444.
- [19] P. J. Peebles, B. Ratra, Reviews of Modern Physics 75 (2003) 559-606.
- [20] L. Perivolaropoulos, Journal of Physics Conference Series 222 (2010) 012024.
- [21] B. Ratra, P. J. E. Peebles, Phys. Rev. D 37 (1988) 3406.
- [22] A. G. Riess, et al. , Astron. J 116 (1998) 1009-1038.
- [23] B. Ratra, Phys. Rev. D 43 (1991) 3802-3812.
- [24] P. J. E. Peebles, B. Ratra, Astrophys. J 325 (1988) L17-L20.
- [25] H. K. Jassal, J. S. Bagla, T. Padmanabhan, Mon. Not. R. Astron. Soc. 405 (2010) 2639-2650.
- [26] K. M. Wilson, G. Chen, B. Ratra, Modern Physics Letters A 21 (2006) 2197-2204.
- [27] T. M. Davis, et al. , Astrophys. J 666 (2007) 716-725.
- [28] S. W. Allen, et al. , Mon. Not. R. Astron. Soc. 383 (2008) 879-896.
- [29] S. Perlmutter, et al. , Astrophys. J 517 (1999) 565-586.
- [30] A. Shafieloo, V. Sahni, A. A. Starobinsky, Phys. Rev. D 80 (2009) 101301.
- [31] T. Holsclaw, et al. , Physical Review Letters 105 (2010) 241302.
- [32] B. Ratra, et al. , Astrophys. J 517 (1999) 549-564.
- [33] S. Podariu, et al. , Astrophys. J 559 (2001) 9-22.
- [34] D. N. Spergel, et al. , ApJS 148 (2003) 175-194.
- [35] E. Komatsu, et al. , ApJS 180 (2009) 330-376.
- [36] E. Komatsu, et al. , ApJS 192 (2011) 18-+.
- [37] G. Chen, B. Ratra, Publ.Astron.Soc.Pac. 115 (2003) 1143-1149.
- [38] W. J. Percival, et al. , Mon. Not. R. Astron. Soc. 381 (2007) 1053-1066.
- [39] E. Gaztañaga, A. Cabré, L. Hui, Mon. Not. R. Astron. Soc. 399 (2009) 1663-1680.
- [40] L. Samushia, B. Ratra, Astrophys. J 701 (2009) 1373-1380.
- [41] Y. Wang, Modern Physics Letters A 25 (2010) 3093-3113.
- [42] S. Podariu, P. Nugent, B. Ratra, Astrophys. J 553 (2001) 39-46.
- [43] L. Samushia, et al. , Mon. Not. R. Astron. Soc. 410 (2011) 1993-2002.
- [44] Y. Wang, et al. , Mon. Not. R. Astron. Soc. 409 (2010) 737-749.

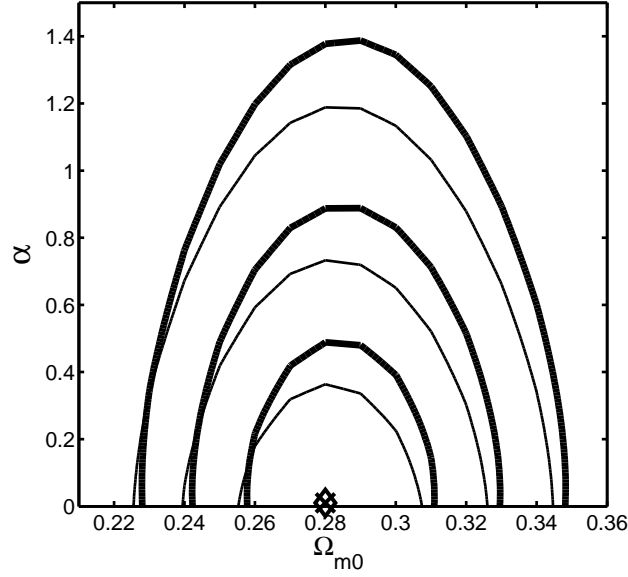


FIG. 8: Thick (thin) solid lines are 1, 2, and 3  $\sigma$  constraint contours for the  $\phi$ CDM model from a joint analysis of the BAO and SNeIa (with systematic errors) data, with (and without) the ADD data. The cross (“x”) marks the best-fit point determined from the joint sample without the ADD data at  $\Omega_{m0} = 0.28$  and  $\alpha = 0$  with  $\chi^2_{\min} = 531$ . The diamond (“ $\diamond$ ”) marks the best-fit point determined from the joint sample with the ADD data at  $\Omega_{m0} = 0.28$  and  $\alpha = 0.01$  with  $\chi^2_{\min} = 572$ . The  $\alpha = 0$  horizontal axis corresponds to spatially-flat  $\Lambda$ CDM models.

- [45] L. Samushia, B. Ratra, ApJL 680 (2008) L1-L4.
- [46] S. Ettori, et al. , Astron.Astrophys. 501 (2009) 61-73.
- [47] B. E. Schaefer, Astrophys. J 660 (2007) 16-46.
- [48] N. Liang, S. N. Zhang, in: American Institute of Physics Conference Series, volume 1065 of American Institute of Physics Conference Series, pp. 367-372.
- [49] Y. Wang, Phys. Rev. D 78 (2008) 123532.
- [50] L. Samushia, B. Ratra, Astrophys. J 714 (2010) 1347-1354.
- [51] J. Courtin, et al. , Mon. Not. R. Astron. Soc. 410 (2011) 1911-1931.
- [52] M. Baldi, Astron. J 411 (2011) 1077-1103.
- [53] S. Basilakos, M. Plionis, J. Sola, Phys. Rev. D 82 (2010) 083512.
- [54] K.-H. Chae, et al. , Phys. Rev. Lett. 89 (2002) 151301.
- [55] K.-H. Chae, et al. , ApJL 607 (2004) L71-L74.
- [56] S. Lee, K.-W. Ng, Phys. Rev. D 76 (2007) 043518.
- [57] M. Yashar, et al. , Phys. Rev. D 79 (2009) 103004.
- [58] S. Capozziello, et al. , Phys. Rev. D 70 (2004) 123501-+.
- [59] J. Simon, L. Verde, R. Jimenez, Phys. Rev. D 71 (2005) 123001.
- [60] L. Samushia, et al. , Physics Letters B 693 (2010) 509-514.
- [61] M. A. Dantas, et al. , Physics Letters B 699 (2011) 239-245.
- [62] L. Samushia, B. Ratra, ApJL 650 (2006) L5-L8.
- [63] L. Samushia, G. Chen, B. Ratra, arXiv:0706.1963.
- [64] E. Fernandez-Martinez, L. Verde, JCAP 8 (2008) 23.
- [65] R.-J. Yang, S. N. Zhang, Mon. Not. R. Astron. Soc. 407 (2010) 1835-1841.
- [66] L. I. Gurvits, K. I. Kellermann, S. Frey, Astron. Astrophys. 342 (1999) 378-388.
- [67] E. J. Guerra, R. A. Daly, L. Wan, Astrophys. J 544 (2000) 659-670.
- [68] G. Chen, B. Ratra, Astrophys. J 582 (2003) 586-589.
- [69] S. Podariu, et al. , Astrophys. J 584 (2003) 577-579.
- [70] D. L. Khokhlov, Int. J Mod. Phys. D 20 (2011) 1167-1169.
- [71] F. de Bernardis, E. Giusarma, A. Melchiorri, International Journal of Modern Physics D 15 (2006) 759-766.
- [72] R. F. L. Holanda, J. V. Cunha, J. A. S. Lima, arXiv:0807.0647.
- [73] J. A. S. Lima, R. F. L. Holanda, J. V. Cunha, in: American Institute of Physics Conference Series, volume 1241 of American Institute of Physics Conference Series, pp. 224-229.
- [74] Z. Li, P. Wu, H. Yu, ApJL 729 (2011) L14.
- [75] N. Liang, S. Cao, Z.-H. Zhu, arXiv:1104.2497.

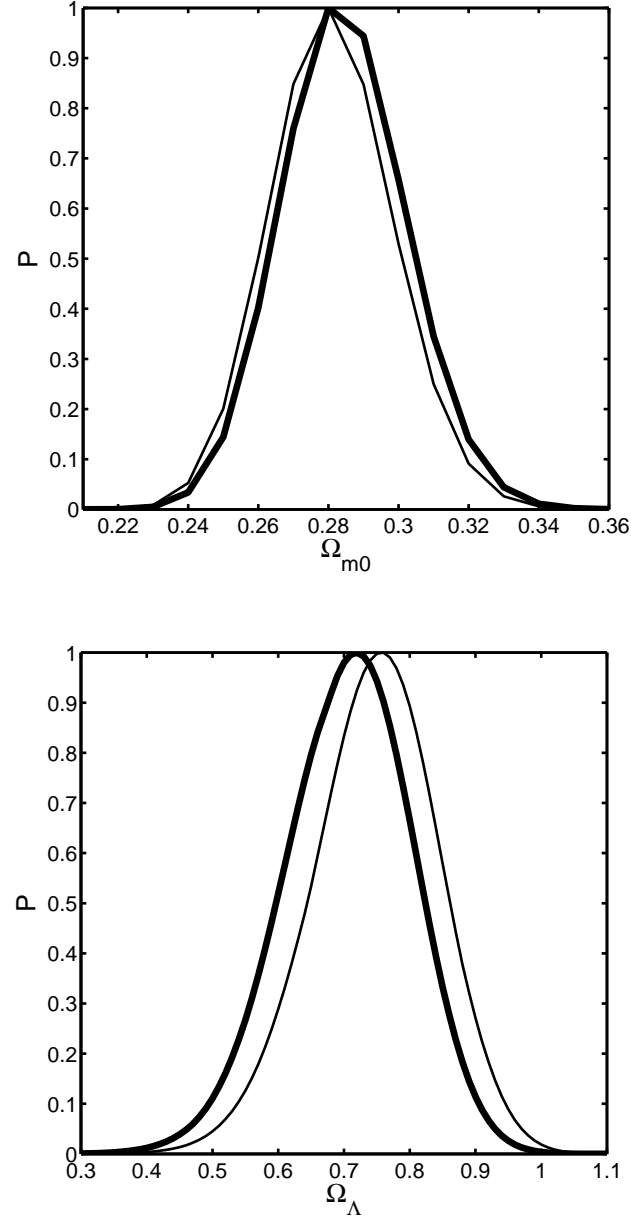


FIG. 9: One-dimensional marginalized distribution probabilities of the cosmological parameters for the LCDM model. Thick (thin) lines are results from a joint analysis of the BAO and SNeIa (with systematic errors) data, with (and without) the ADD data.

- [76] X.-L. Meng, T.-J. Zhang, H. Zhan, arXiv:1104.2833.
- [77] G. Chen, J. R. Gott, III, B. Ratra, Publ. Astron. Soc. Pac. 115 (2003) 1269-1279.
- [78] W. J. Percival, et al. , Mon. Not. R. Astron. Soc. 401 (2010) 2148-2168.
- [79] L. Samushia, B. Ratra, Astrophys. J 703 (2009) 1904-1910.
- [80] D. J. Eisenstein, et al. , Astrophys. J 633 (2005) 560-574.
- [81] R. Amanullah, et al. , Astrophys. J 716 (2010) 712-738.
- [82] E. di Pietro, J.-F. Claeskens, Mon. Not. Roy. Astron. Soc. 341 (2003) 1299-1310.
- [83] L. Perivolaropoulos, Phys. Rev. D 71 (2005) 063503.
- [84] S. Nesseris, L. Perivolaropoulos, Phys. Rev. D 72 (2005) 123519.
- [85] M. Kowalski, et al. , Astrophys. J 686 (2008) 749-778.

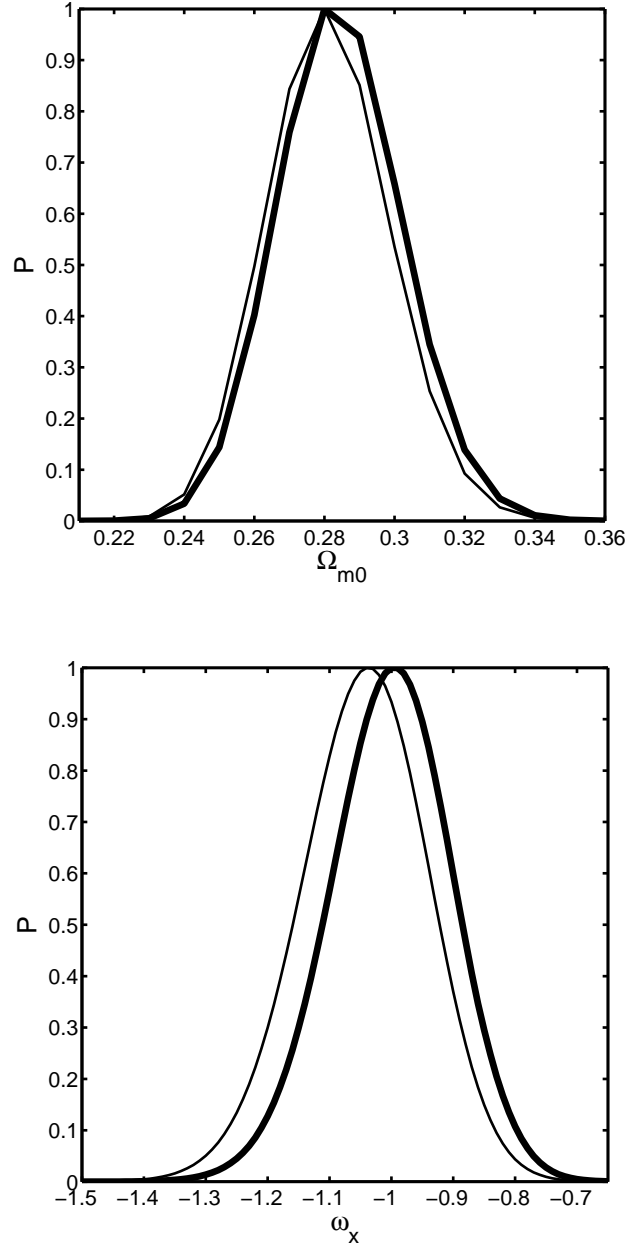


FIG. 10: One-dimensional marginalized distribution probabilities of the cosmological parameters for the XCDM parametrization. Thick (thin) lines are results from a joint analysis of the BAO and SNeIa (with systematic errors) data, with (and without) the ADD data.

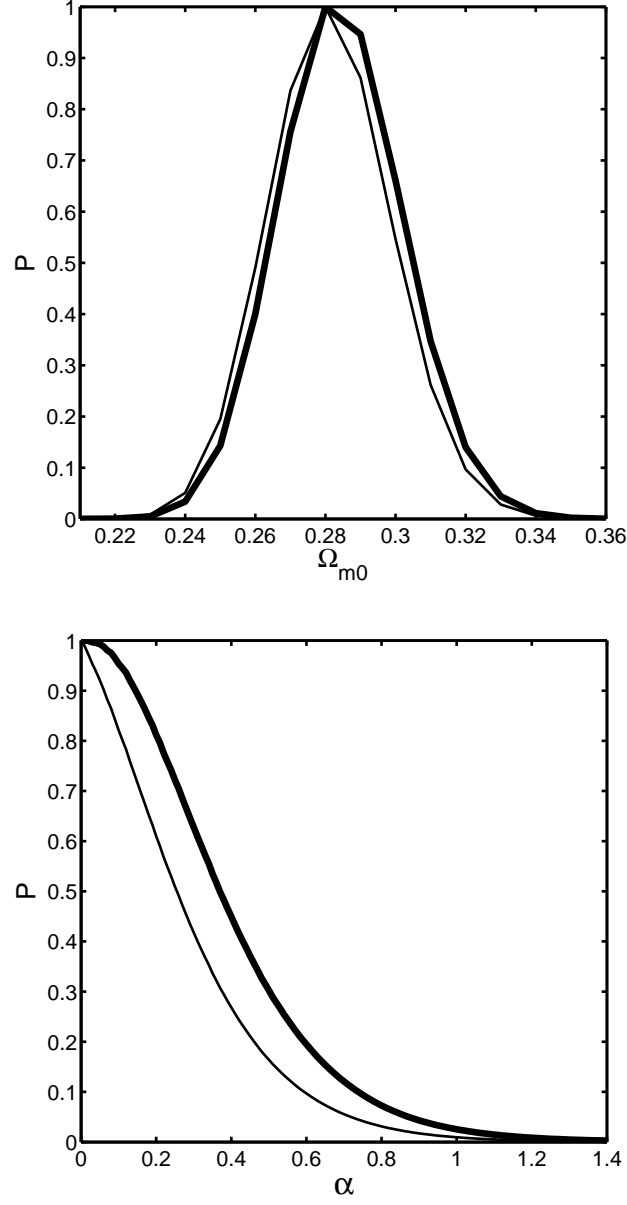


FIG. 11: One-dimensional marginalized distribution probabilities of the cosmological parameters for the  $\phi$ CDM model. Thick (thin) lines are results from a joint analysis of the BAO and SNeIa (with systematic errors) data, with (and without) the ADD data.